



FLUID-STRUCTURE INTERACTION WITH VISCOELASTICITY IN NUMERICAL SIMULATION OF WATER HAMMER

MESSAOUDENE B. ^{1*}, FERROUK M. ²

^{1,2} Mouloud Mammeri University of Tizi Ouzou, Laboratory of Energy, Mechanics and Materials (LEMM), 15000, Algeria

(* *boualem.messaoudene@fgc.ummto.dz*)

Research Article – Available at <http://larhyss.net/ojs/index.php/larhyss/index>
Received February 16, 2024, Received in revised form May 27, 2024, Accepted June 2, 2024

ABSTRACT

This paper presents the numerical simulation of water hammer considering the mechanical rheological behavior of plastic pipes, HDPE (high density polyethylene) or PVC (polyvinyl chloride), involving transient liquid flows. In past or current applications based on the incorporation of unsteady friction, it has been widely observed that pressure damping effects are not sufficient to correctly predict the experimental data. Therefore, to solve this problem, it becomes important to also add the deformation effects of the selected pipe wall material. The detailed analysis of the viscoelastic model shows that the creep function deserves special attention: the parameters J_k (creep compliance) and τ_k (retarded time) must be well calibrated to obtain a perfect match between the laboratory data and the numerical results. Apart from these sometimes over-demanding concerns, the incorporation of the viscoelastic model seems sufficient to compensate for the pressure damping that eludes other traditional friction models such as the Brunone and Vardy-Brown models.

Keywords: Water hammer, Hydraulic transient, Wave propagation, MOC, Viscoelasticity.

ABBREVIATION

| | |
|-----|---|
| H | Piezometric head (m) |
| Q | Discharge (m^3/s) |
| x | Coordinate along the pipeline axis in (m) |
| t | Time (s) |
| L | Length of the pipeline (m) |
| D | Pipe inner diameter (m) |
| A | Cross-sectional area (m^2) |
| e | Pipe-wall thickness (m) |

| | |
|-----------------|---|
| g | Gravity due to acceleration (m/s^2) |
| a | Wave celerity in (m/s) |
| E_0 | Young's modulus of elasticity of the pipe (Pa) |
| K | Fluid bulk modulus (Pa) |
| α | Parameter dependent on Poisson's ratio and type of pipe anchorage |
| ν | Poisson's ratio |
| h_{fs} | Quasi-steady friction |
| h_{fu} | Unsteady friction |
| f_s | Darcy-Weisbach steady-state friction factor (-) |
| J | Creep compliance function of pipe wall material (Pa^{-1}) |
| J_k | Creep compliance parameter of pipe wall material (Pa^{-1}) |
| τ_k | Retarded time (s) |
| ε_r | Retarded strain is expressed using the Kelvin–Voigt model (KV) |
| σ | Circumferential stress (Pa) |
| ε | Circumferential total strain (-) |
| ε_e | Circumferential elastic strain (-) |
| ε_r | Circumferential retarded strain (-) |
| N_{KV} | Number of each Kelvin–Voigt element |
| C_p, C_n, C_a | Coefficients used in the method of characteristics (MOC) |
| T_v | Valve closing time |
| H_{V0} | Steady-state piezometric head at downstream valve |
| PE | polyethylene |
| HDPE | High-density polyethylene |
| LDPE | Low-density polyethylene |
| PVC | Polyvinyl chloride |
| MOC | Method of characteristics |
| AB | Acceleration based - models |
| CB | Convolution based - models |
| MAPE | Mean Absolute Percentage Error |

INTRODUCTION

Transient flows are very common in practice, and are encountered in many situations such as hydraulic systems, pressurized piping systems, water supply systems and heating or cooling systems in nuclear power plants. They are the cause of flow variations that occur, for example, when a shut-off valve is opened or closed very quickly, or when a pump is started or stopped suddenly. Sometimes, they also occur following a power cut that must supply the pump or other operating equipment in the hydraulic network. In such situations, a phenomenon commonly known as water hammer occurs, causing strong oscillations in the pressure waves behind it, which can seriously impair the smooth running of the system (Chaudhry, 1979; Wylie and Streeter, 1993).

In many reviews of articles devoted to the phenomenon of water hammer, a key question is often asked concerning the correct modelling of the instantaneous wall shear stress. In the case of hydraulic systems made of plastic pipes such as PVC or HDPE, the approach to be followed differs somewhat from that usually applied to steel or copper pipes. This is the subject of our article here.

In this paper, an extension of the method of characteristics (MOC) is presented to show how to include the viscoelastic mechanical behavior of the pipe in the continuity equation of the Water hammer problem. With such modifications, the effects of frictional energy losses are better taken into account (Aklonis et al., 1972; Covas et al., 2004, 2005; Soares et al., 2008; Keramat et al., 2013; Triki, 2016). This approach involves an additional term corresponding to an instantaneous derivative of the delayed deformation of the pipe wall. In the literature, several studies have been performed and discussed regarding the low pressure attenuation observed when applying the classical elastic models: (i) Quasi-steady friction model, (ii) unsteady friction model.

In fact, there are two ways to present the unsteady friction that occurs in a long hydraulic pipe. First, Vitkovsky et al. (2000) and Bergant et al. (2001) carefully studied and analyzed the formula of Brunone et al. (1991). This approach based on the instantaneous acceleration of the local flow is implemented in several commercial software (AFT IMPULSE) because it is relatively easy to implement in the form of a computer program unlike other models, but also because it requires less memory storage and therefore runs quickly. Then, we have the convolution based models such as: (i) Zielke's model (1968) - applicable to the laminar regime of transient flows, (ii) Trikha's model (1975) - which represents a simplification of Zielke's formula, (iii) Vardy and Brown's model (1995, 2003, 2004) - considered as the most recommended because it not only preserves the phase, but also better reproduces the shape of pressure peaks.

By analogy, elastic models depend on the weighting function (Zielke, 1968). However, viscoelastic models use the creep compliance function of the pipe wall (Aklonis et al., 1972). Therefore, both models depend on the flow history. A clarification regarding convolution, many complex physical problems make use of this trick. From a mathematical point of view, convolution is based on a very sound intuitive theorem. Convolution of signals and convolution of images using filters are very good examples.

The main objective of this paper is to present an accurate and critical comparison of the numerical results obtained by applying the classical elastic model and the new viscoelastic approach to an experiment published by Covas et al. (2004). First, two unsteady elastic models Brunone et al. (1991) and Vardy and Brown (2003) are chosen to perform this work. Then, the viscoelastic model is applied and the results are discussed and analyzed with particular emphasis on the stress-strain and its necessary calibration parameters J_k (Creep coefficients) and τ_k (retarded time).

MATHEMATICAL EQUATIONS

The equations governing the modeling of hydraulic transients in pressurized pipes are described below. The convection terms are neglected, the unsteady friction term and the viscoelastic mechanical deformation are integrated in the problem (Covas e al., 2004; Soares et al., 2008; Keramat et al., 2013):

$$\frac{\partial H(x,t)}{\partial t} + \frac{a^2}{gA} \frac{\partial Q(x,t)}{\partial x} + 2 \frac{a^2}{g} \frac{\partial \varepsilon_r(x,t)}{\partial t} = 0 \quad (1)$$

$$\frac{1}{A} \frac{\partial Q(x,t)}{\partial t} + g \frac{\partial H(x,t)}{\partial x} + g(h_{f_s} + h_{f_u}) = 0 \quad (2)$$

with H the piezometric head in m, Q the flow discharge in m^3/s , g the gravity acceleration m/s^2 , A the cross-sectional area of the pipe in m^2 , x the coordinate along the pipeline axis in m, t the time in s, $a^2 = (K/\rho)/(1 + \alpha * D/e * K/E_0)$ the wave celerity in m/s, D the pipe inner diameter in m, e the pipe-wall thickness in m, ρ the density in kg/m^3 , K bulk modulus of elasticity of the fluid in Pa, E_0 Young's modulus of elasticity of the pipe in Pa, α the Poisson's ratio dependent parameter (Wylie and Streeter, 1993). The steady friction term $h_{f_s} = f_s Q|Q|/(2gDA^2)$ is calculated by the Colebrook-White formula. The unsteady friction term for model of Brunone $h_{f_u} = (k/gA) (\partial Q/\partial t + aSGN(Q)\partial Q/\partial x)$ (Vitkovsky et al., 2000; Bergant et al., 2001) and for model of Vardy and Brown (2003), see APPENDIX A. The retarded strain ε_r is expressed using the following Kelvin–Voigt model (Covas et al., 2005):

$$\varepsilon_r(x, t) = \sum_{k=1}^{N_{KV}} \frac{\alpha D \rho g}{2e} \int_0^t \{H(x, t - s) - H(x, 0)\} \frac{J_k}{\tau_k} e^{-\frac{s}{\tau_k}} ds \quad (3)$$

with $\sigma = \alpha \Delta P D / 2e$ is the circumferential-stress in Pa, $\Delta P = \rho g \{H(x, t - s) - H_0(x, t - s)\}$ in Pa, $\varepsilon_e = \sigma / E_0$ is the elastic circumferential strain, and total circumferential strain is given by Aklonis et al. (1972):

$$\varepsilon(x, t) = \varepsilon_e(x) + \varepsilon(x, t) = \sigma J_0 + \int_{t=0}^t \sigma(x, t - s) \frac{\partial J(x, s)}{\partial s} ds \quad (4)$$

The creep function is described as follows (Aklonis et al., 1972; Keramat et al., 2013):

$$J(x, t) = J(x, 0) + \sum_{k=1}^{N_{KV}} J_k \left(1 - e^{-\frac{t}{\tau_k}} \right) \quad (5)$$

The time derivative of the retarded deformation (Eq. 3) can be obtained by the analytical differentiation method presented in the appendix by Covas et al. (2005):

$$\frac{\partial \varepsilon_r(x,t)}{\partial t} = \sum_{k=1}^N \left[\frac{J_k}{\tau_k} \frac{\alpha D \rho g}{2e} \{H(x, t - s) - H(x, 0)\} - \frac{\varepsilon_{rk}(x,t)}{\tau_k} \right] \quad (6)$$

Equations (1) and (2) are transformed into a system of ordinary differential equations with respect to time only by the method of characteristics described as follows:

$$\frac{dH(x,t)}{dt} \pm \frac{a}{gA} \frac{dQ(x,t)}{dt} + \frac{2a^2}{g} \frac{d\varepsilon_r(x,t)}{dt} \pm a(h_{f_s} + h_{f_u}) = 0 \quad (7)$$

Applying the first order finite difference method in space and the first explicit scheme in time, we obtain:

$$C^+: Q(x, t) = C_p - C_a H(x - \Delta x, t) \quad (8)$$

$$C^-: Q(x, t) = C_n + C_a H(x + \Delta x, t) \quad (9)$$

$$C_p = Q(x - \Delta x, t - \Delta t) + C_a H(x - \Delta x, t - \Delta t) + \Delta t \left(-2Aa \frac{\partial \varepsilon_r}{\partial t} - gAh_f \right) \quad (10)$$

$$C_n = Q(x + \Delta x, t - \Delta t) - C_a H(x + \Delta x, t - \Delta t) + \Delta t \left(+2Aa \frac{\partial \varepsilon_r}{\partial t} - gAh_f \right) \quad (11)$$

$$C_a = gA/a \quad (12)$$

At the internal nodes (see Fig. 1), a simultaneous solution of linear equations (8) and (9), gives us the variables $H(x, t)$ and $Q(x, t)$ at the present instant, knowing already their values at the previous instant. The coefficients C_p and C_n are therefore defined at time $t - \Delta t$. Several boundary conditions are exposed in these articles (Chaudhry, 1979; Wylie and Streeter, 1993).

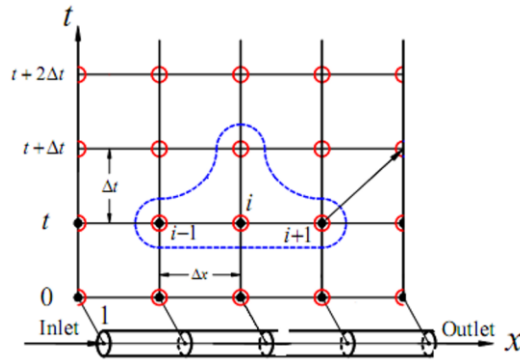


Figure 1: Rectangular grid of characteristics

NUMERICAL RESULTS

In the literature (Covas et al., 2004, 2005; Soares et al., 2008; Keramat et al., 2013; Triki, 2016), the experimental creep curve is obtained by following the inverse calculation procedure or simply by tensile and compressive creep tests on one or more polymer samples. In several experiments, wave celerity between 350 and 450 m/s were tested to better account for the strain rate. In principle, a single creep curve should correspond to each test. Then, for numerical purposes, the creep coefficients J_k and τ_k can be determined using the least squares procedure of the Levenberg algorithm. The creep

function modeled as a series of several exponentials was found to be very effective in reproducing the input data set correctly. As an initial parameter, the creep coefficient J_0 corresponding to the inverse of the Young's modulus E_0 must be imposed before starting the least squares procedure.

In this work, the data collected in this paper (Covas et al., 2004) at location T1 (see Fig. 2), near the valve located 271 m from the high-pressure tank (Air Vessel), are presented in Table 1. In contrast, the new calibrated creep parameters J_k and τ_k are presented in Table 2.

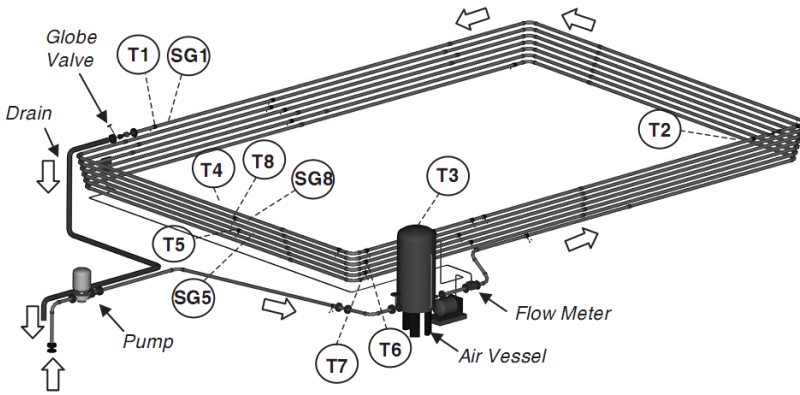


Figure 2: Imperial College experimental facility, London

Table 1: Experimental data performed by Covas et al. (2004, 2005)

| L | D | e | E | ν | Q_0 | H_0 | T_v |
|-------|---------|--------|----------|-------|----------|-------|--------|
| 277 m | 50.6 mm | 6.3 mm | 1.27 GPa | 0.46 | 1.01 l/s | 45 m | 0.09 s |

Table 2: New calibrated parameters for the creep coefficient J_k and delay time τ_k with $Q_0=1.0(l/s)$

| a (m/s) | J_0 | (τ_k, J_k) | | | |
|-----------|-------|--|------------------|------------------|------------------|
| | | τ_k in (s) ; J_k in ($10^{-9} Pa^{-1}$) | | | |
| | | (τ_1, J_1) | (τ_2, J_2) | (τ_3, J_3) | (τ_4, J_4) |
| 372 | 0.79 | (0.0500, 0.0259) | (0.5000, 0.0712) | (1.5001, 0.1360) | (10.000, 0.4648) |
| 381 | 0.75 | (0.0932, 0.0187) | (0.4932, 0.0605) | (1.3726, 0.1354) | (9.1731, 0.4404) |
| 394 | 0.70 | (0.1752, 0.0388) | (1.0553, 0.1592) | (6.3123, 0.0679) | (8.5282, 0.3516) |
| 410 | 0.64 | (0.0826, 0.0370) | (0.9204, 0.1587) | (7.0333, 0.2008) | (7.1073, 0.1874) |
| 426 | 0.59 | (0.3945, 0.1135) | (1.6342, 0.0895) | (6.2501, 0.3344) | (9.0713, 0.0000) |

In contrast to the elastic models presented in Figure 3 Quasi-steady, Brunone et al. (1991) and Vardy-Brown (2003), the viscoelastic approach currently proposed therefore proves highly effective in better absorbing high hydraulic pressures in pressurized HDPE pipes. It should also be remembered that recent studies carried out on hydraulic systems composed mainly of steel or copper pipes have led to the following conclusions:

1. The quasi-steady model is too simplified to be applied to transient flows.
2. Brunone's model, based on instantaneous acceleration, gives an inappropriate form to pressure peaks, due to the difficulty of correctly estimating the empirical decay coefficient k that enters its equation.
3. In contrast to the other approaches, models based on integral convolution (BC) predict the profile of measured pressure waves almost perfectly.

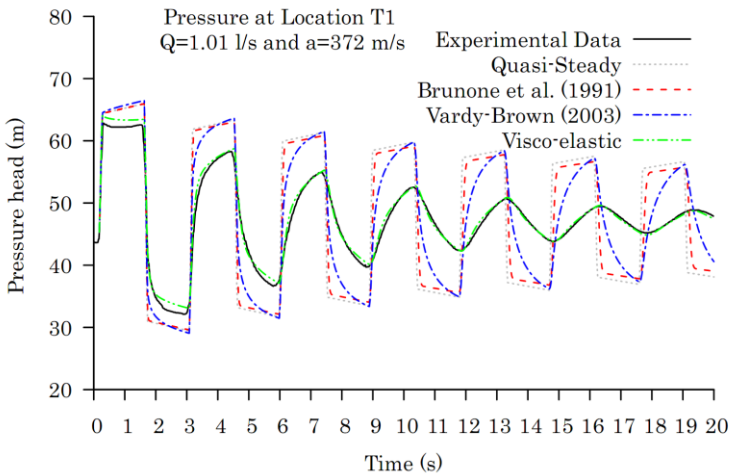


Figure 3: Piezometric head profiles at location T1 for $Q=1.01$ l/s and $a=372$ m/s

In Fig. 4, three wave velocities have been selected to show the effects induced on pressure phase shift and damping ratio. In this case, only the viscoelastic model was simulated. It can be seen that the observed shift is more closely related to phase-shift problems, which do indeed require an appropriate choice of pressure wave velocity. Physically, this appropriate choice of pressure wave velocity can be interpreted as the result of the margin of error of the experimentally transmitted frequency band, or sometimes of the exact location of the pressure transducer due to the stability condition that must be satisfied.

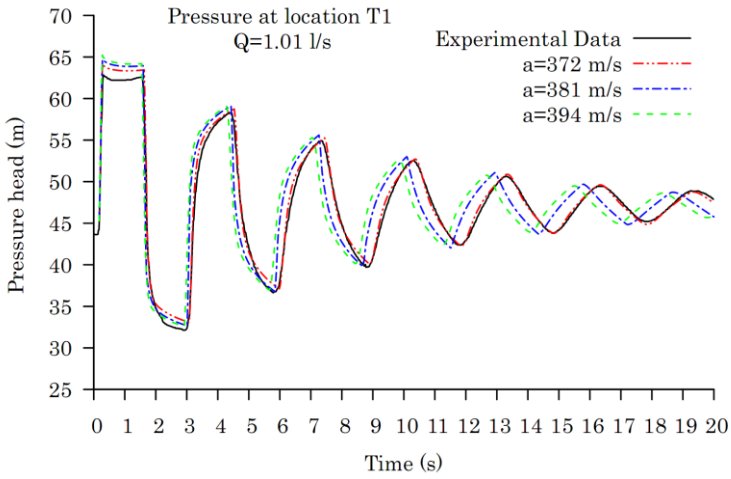


Figure 4: Piezometric head profiles at location T1 for $Q=1.01$ l/s and various wave velocity

As a viscoelastic material, the inherent nature of HDPE's mechanical and viscoelastic properties means that it often undergoes time-dependent deformation (strain), as shown in Fig. 5. Throughout the simulation, the magnitude of the offset between total and delayed deformation is very large. The offset between these two deformation profiles can be represented by elastic deformation (elastic-strain), which can be easily estimated using a fixed initial Young's modulus.

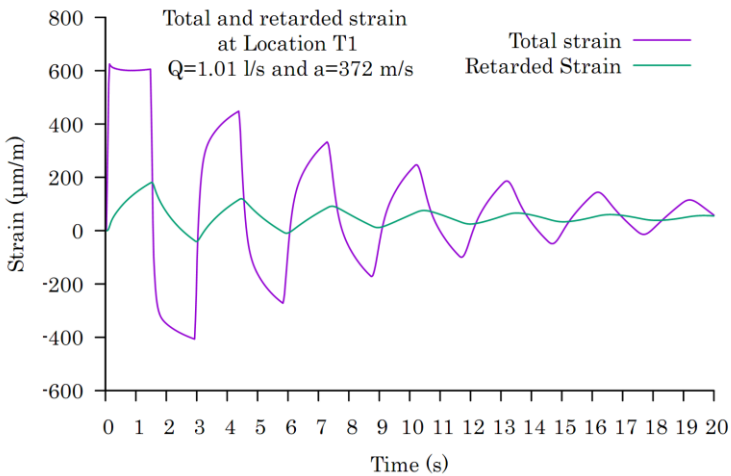


Figure 5: Numerical results (total and retarded strain) of viscoelastic transient at location 1 for $Q=1.01$ l/s and $a=372$ m/s

In Fig. 6, a wave velocity nuance was illustrated by describing creep as a function of time for high and low density polyethylene. At the initial time, all creep curves start at J_0 and end up marking their respective depths at the final time, defined in the upper right corner. Therefore, the lower the celerity, the higher the creep, which results in a larger deformation in that direction. On the other hand, the creep becomes a critical parameter to fit the numerical data with better accuracy. The analysis established on the basis of phase shift and pressure attenuation effects allowed to find a compromise for the wave velocity $a=372$ m/s. On the other hand, even with a simple choice made from Table 2 or Fig. 6, the viscoelastic transient model often gives an acceptable fit compared to the classical elastic model. Strictly speaking, the major drawback is more related to the phase shift than to the pressure attenuation effects. If we continue our analysis at higher speeds, we encounter other types of polymers such as nylon, polyester, PVC and finally steel at the last line where the creep is zero and the wave velocity close to 1300 m/s.

In the literature, it is also mentioned that the wave velocity depends essentially on the initial Young's modulus E_0 . For example, if we take the case of a PE pipe illustrated in Fig. 6, the wave velocity varies between 372 and 426 m/s, corresponding to an initial Young's modulus ranging from 1.27 to 1.69 GPa. In the case of a PVC pipe, on the other hand, the velocity varies between 411 and 440 m/s, corresponding respectively to a Young's modulus of between 2.40 and 2.75 GPa (Soares et al., 2008). Covas et al. (2004, 2005) have shown that wave velocity is a time-dependent function in transient flow, due not only to the effects of unsteady friction and fluid inertias, but also to the viscoelastic and rheological behavior inherent in the pipe wall.

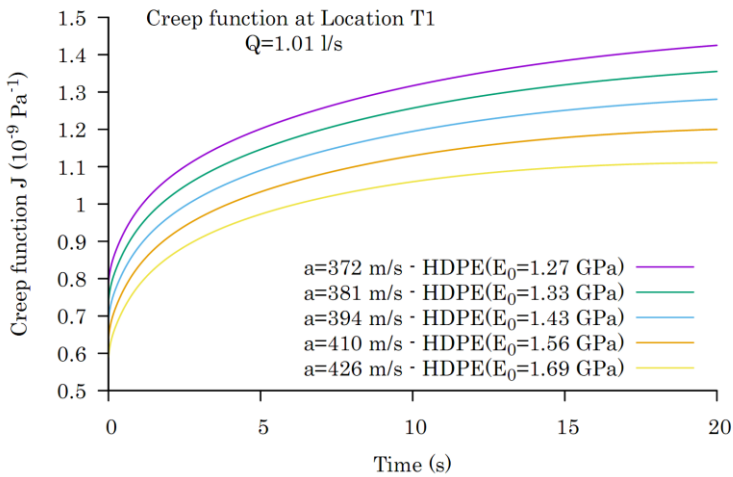


Figure 6: Creep function profiles for several Young's modulus Initial for $Q=1.01$ l/s and $a=372$ m/s

According to the quantitative analysis of pressure attenuation (Pressure decrease rate), the mean absolute percentage error MAPE, widely used in a comparison process, is too glaring for the classical friction models presented, namely an error of over 18.76% for the

quasi-steady model, 16.63% for Brunone and 12.91% for Vardy-Brown (see figure 3). In contrast to these friction-based models, viscoelasticity shows a significant improvement, with a mean absolute error of less than 1.09%. The comparison was carried out over the entire interval $t = [0, 20]$ for $n=1195$ observations.

$$MAPE = \frac{1}{n} \sum_{i=1}^n \left| \frac{Pe_i - P_i}{Pe_i} \right| \tag{13}$$

where n is the number of values observed over time, Pe_i and P_i represent the observation and prediction data respectively.

The E_t parameter describes the proposed method for estimating the relative errors between measured and numerically calculated frequencies (see figure 4). The 13 points Te_i and T_i , corresponding respectively to the half-period of each measured and calculated oscillation, are obtained by the intersection between the straight line $y = H_{V0}$ and the experimental or numerical data set. The relative errors evaluated are summarized in Table 3. Analysis of these data shows that the appropriate wave velocity is indeed closer to 372m/s. In summary, the frequency error increases more with higher wave velocity.

$$E_t = \frac{1}{n} \sum_{i=1}^n \left| \frac{Te_i - T_i}{Te_i} \right| \tag{14}$$

where Te_i and T_i represent respectively the observation and prediction data to the half-period of each oscillation.

Table 3: Mean relative frequency errors

| a (m/s) | 372 | 381 | 394 | 410 | 426 |
|-----------|------|------|------|------|------|
| E_t (%) | 0.20 | 3.50 | 5.40 | 7.10 | 8.80 |

CONCLUSION

In this paper, we have shown how to accurately calibrate the creep function with respect to Young's modulus when water flows transiently through a high density PHD pipe. Although the linear viscoelastic model, as illustrated, appears to give good agreement with the experimental data and therefore better describes the effects of pressure attenuation in terms of pressure oscillations, the process of calculating creep parameters remains highly criticized due to the dependence of these creep parameters on reference data. Consequently, this process does not necessarily lead to generalizable results and will depend always on some benchmark experiments. This is the main drawback of the linear viscoelastic model. During the multiple wave celerity simulations, we also found that the period of oscillation decreased as the velocity increased. Therefore, a slight manipulation of the CFL (Courant-Friedrichs-Lewy) condition allows us to obtain a more accurate oscillation period. Finally, the numerical results obtained were found to be consistent with the experimental data encountered in the literature.

Declaration of competing interest

The authors declare that they have no known competing financial interests or personal relationships that could have appeared to influence the work reported in this paper.

Acknowledgements

This work was supported by the Laboratory of Energy, Mechanics and Materials (LEMM), University of Tizi Ouzou, Algeria.

APPENDIX A: Description of quasi-steady and unsteady friction models

In this appendix, quasi-steady and unsteady elastic models are presented to show how wall shear stress has been modeled. First, let's recall the momentum equation:

$$\frac{1}{A} \frac{\partial Q(x,t)}{\partial t} + g \frac{\partial H(x,t)}{\partial x} + g(h_{f_s} + h_{f_u}) = 0$$

The quasi-steady friction term is calculated by the Colebrook-White formula:

$$h_{f_s} = f_s \frac{Q|Q|}{2gDA^2}$$

where f_s is the Darcy friction coefficient which can be calculated according to the flow regime:

For transient laminar flow ($Re \leq 2300$), the Hagen-Poiseuille law is used:

$$f_s = 64/Re.$$

For transient turbulent flow ($Re > 2300$), the Colebrook-White formula as:

$$\frac{1}{\sqrt{f_s}} = -2 \log \left(\frac{2.51}{Re \sqrt{f_s}} + \frac{\varepsilon/D}{3.71} \right)$$

The unsteady friction term presented by Brunone et al. (1991):

$$h_{f_u} = \frac{k}{gA} \left(\frac{\partial Q}{\partial t} + a \operatorname{SGN}(Q) \frac{\partial Q}{\partial x} \right)$$

where k = empirical decay coefficient, and $\operatorname{SGN}(Q) = \operatorname{abs}(Q)/Q$. This sign of the average discharge (SGN operator) was introduced by Vitkovsky et al. (2000).

The unsteady friction term based on integral-convolution (Zielke, 1968):

$$h_{f_u} = \frac{16\nu}{gD^2A} \int_0^t \frac{\partial Q}{\partial t}(u) W(t-u) du$$

The Vardy-Brown weighting function is given by Vardy and Brown (1995, 2003):

$$W(\tau) = \frac{A^* e^{-\tau/C^*}}{\sqrt{\tau}}$$

where

$$A^* = 1/\sqrt{2\pi}, C^* = 12.86/Re^k, k = \log_{10}(15.29/Re^{0.0567})$$

The simulations carried out using these models lead to the following conclusions:

- Brunone's model depends on the empirical decay coefficient k , which makes it difficult to generalize. It does, however, have the advantage of being quick to run.
- The Vardy-Brown model is very practical in the case of a rapidly evolving velocity field. However, it has the disadvantage of running very slowly.
- In plastic pipes, the combination of Vardy and Brown's formula and the viscoelastic term introduced in the continuity equation generally gives very appreciable results.

REFERENCES

- AKLONIS J.J., MACKNIGHT W.J., SHEN M. (1972). Introduction to Polymer Viscoelasticity. John Wiley & Sons, Inc, NewYork.
- BERGANT A., ROSS SIMPSON A., VITKOVSKY J. (2001). "Developments in unsteady pipe flow friction modelling," Journal of Hydraulic Research, Vol. 39, No 3, pp. 249–257. <https://doi.org/10.1080/00221680109499828>
- BRUNONE B., GOLIA U.M., GRECO M. (1991). Modelling of fast transients by numerical methods, in: E. Cabrera, M. Fanelli (Eds.), Proc., Int. Meeting on Hydraulic Transients and Water Column Separation, Valencia, pp. 273-280.
- CHAUDHRY M.H. (1979). Applied Hydraulic Transients. Van Nostrand Reinhold.
- COVAS D., STOIANOV I., RAMOS H., GRAHAM N., MAKSIMOVIC C. (2004). "The dynamic effect of pipe-wall viscoelasticity in hydraulic transients. Part I—experimental analysis and creep characterization," Journal of Hydraulic Research, Vol. 42, No 5, pp. 517–532. <https://doi.org/10.1080/00221686.2004.9641221>
- COVAS D., STOIANOV I., MANO J.F., RAMOS H., GRAHAM N., MAKSIMOVIC C. (2005). "The dynamic effect of pipe-wall viscoelasticity in hydraulic transients. Part II—model development, calibration and verification," Journal of Hydraulic Research, Vol. 43, No 1, pp. 56–70. <https://doi.org/10.1080/00221680509500111>
- KERAMAT A., KOLAH I.A.G., AHMADI A. (2013). "Waterhammer modelling of viscoelastic pipes with a time-dependent Poisson's ratio," Journal of Fluids and Structures, vol. 43, pp. 164–178. <https://doi.org/10.1016/j.jfluidstructs.2013.08.013>

- SOARES A.K., COVAS D. I., REIS L. F. (2008). “Analysis of PVC Pipe-Wall Viscoelasticity during Water Hammer,” *Journal of Hydraulic Engineering*, Vol. 134, No 9, pp. 1389–1394. [https://doi.org/10.1061/\(ASCE\)0733-9429\(2008\)134:9\(1389\)](https://doi.org/10.1061/(ASCE)0733-9429(2008)134:9(1389))
- TRIKHA A.K. (1975). “An Efficient Method for Simulating Frequency-Dependent Friction in Transient Liquid Flow,” *Journal of Fluids Engineering*, Vol. 97, No 1, pp. 97–105. <https://doi.org/10.1115/1.3447224>
- TRIKI A. (2016). “Water-hammer control in pressurized-pipe flow using an in-line polymeric short-section,” *Acta Mechanica*, Vol. 227, No 3, pp. 777–793. <https://doi.org/10.1007/s00707-015-1493-1>
- VARDY A.E., BROWN J.M.B. (2004). “Transient turbulent friction in fully rough pipe flows,” *Journal of Sound and Vibration*, vol. 270, no. 1, pp. 233–257. [https://doi.org/10.1016/S0022-460X\(03\)00492-9](https://doi.org/10.1016/S0022-460X(03)00492-9)
- VARDY A.E., BROWN J.M.B. (2003). “TRANSIENT TURBULENT FRICTION IN SMOOTH PIPE FLOWS,” *Journal of Sound and Vibration*, Vol. 259, No 5, pp. 1011–1036. <https://doi.org/10.1006/jsvi.2002.5160>
- VARDY A.E., BROWN J.M.B. (1995). “Transient, turbulent, smooth pipe friction,” *Journal of Hydraulic Research*, Vol. 33, No 4, pp. 435–456. <https://doi.org/10.1080/00221689509498654>
- VITKOVSKY J.P., LAMBERT M.F, SIMPSON A.R. (2000). “Advances in Unsteady Friction Modelling in Transient Pipe Flow,” *Proceedings of the 8th International Conference on Pressure Surges*. BHR Group Ltd., The Hague, The Netherlands, pp. 471-498.
- WYLIE E.B., STREETER V. L., AND L. SUO (1993). *Fluid Transients in Systems*. Prentice Hall.
- ZIELKE W. (1968). “Frequency-Dependent Friction in Transient Pipe Flow,” *Journal of Basic Engineering*, Vol. 90, No 1, pp. 109–115. <https://doi.org/10.1115/1.3605049>